STUDY OF THERMOLUMINESCENCE CHARACTERISTICS OF QUARTZ FOR HIGH RADIATION DOSES (>1KGY): IMPLICATIONS FOR EXTENDING THE LUMINESCENCE DATING RANGE

Malika Singhal [a,b], Madhusmita Panda [c], S. H. Shinde [d], Sandip Mondal [d], O. Annalakshmi [c,e], Naveen Chauhan [a*]

[a] AMOPH division, Physical Research Laboratory, Navrangpura, Ahmedabad-380009, India

[b] Indian Institute of Technology, Gandhinagar-382355, India

[c] Indira Gandhi Centre of Atomic Research, Kalpakkam, Tamil Nadu-603102, India

[d] Bhabha Atomic Research Centre, Trombay, Mumbai- 400085, India

[e] Homi Bhabha National Institute, IGCAR, Kalpakkam, Tamil Nadu-603102, India

*corresponding author: Email: chauhan@prl.res.in

Abstract

Quartz is an omnipresent abundant natural mineral, used for luminescence dating. Lately, quartz optically stimulated luminescence (OSL) technique is widely used to estimate the equivalent doses (D_e) for dating geological events (up to 250 Gy, limited by saturation). Some works report thermoluminescence (TL) saturation around ~ (10-40) kGy. Still dose estimates for such high radiation dose (HRD) range are not achieved. Significant research exists about luminescence response for low dose ranges (<250 Gy) but limited studies are done for HRDs (>1 kGy). This work characterizes the luminescence response of quartz for HRDs (1-21 kGy) to improve existing understanding of luminescence mechanism. Results show that the characteristics of the trap (<200°C) differ significantly at HRDs than low doses. TL in multi-spectral detection (UV-Visible) band suggest an increase in 340-380°C peak intensity up to 11 kGy dose. The measurements of saturation dose suggest that it depends on the trapping centres but is independent of recombination centres for the samples used for study. The traps are found to be bleachable by sunlight, reducing TL signal to residual levels in 1 hour. Further, the bleachability is found to be anti-correlated with luminescence emission wavelength. At HRDs luminescence sensitivity is influenced by given previous dose which is difficult to correct by routine normalization procedures. The work also explores the normalization method suitable for HRD estimation and recommends the use of mass normalization as other normalization methods do not correct the sensitivity changes at HRDs adequately.

Keywords: Quartz; High dose response; Thermoluminescence; Multispectral; Normalization; Bleachability; previous dose effects

1. INTRODUCTION

Luminescence dating has contributed considerably towards the understanding of the earth surface processes in the late quaternary period (Murray et al., 2021). Quartz and feldspar are two major minerals primarily used in luminescence dating. Feldspar offers to date older sediments but it is prone to anomalous fading and has slow bleachability (Buylaert et al., 2011; Kars et al., 2008). Further, it weathers faster than quartz. In contrast, quartz has excellent bleachability (Murray and Wintle, 2000) and no fading (except for volcanic quartz (Fattahi and Stokes, 2003)) but its age limit is low. The signal in quartz saturates generally around ~250 Gy (Chawla et al., 1998; Huntley et al., 1996; Murray and Wintle, 2000; Wintle and Murray, 2006) compared to feldspar (~2000Gy) (Thiel et al., 2011). Considering stable and fast to bleach signal, quartz is being explored to identify signals suitable for dating older sediments. Protocols such as thermally transferred-optically stimulated luminescence (TT-OSL), violet stimulated luminescence (VSL) (Jain, 2009; Wang et al., 2006) are developed with dose saturation in excess to 1 kGy but with limited success (Ankjærgaard et al., 2016; Duller and Wintle, 2012).

Dosimetric thermoluminescence (TL) peaks of quartz present at temperatures higher than 300°C have a lifetime greater than 10^8 years at ambient temperature of 15°C (Aitken, 1985). Further others have reported greater lifetime such as $1.07*10^{12}$, $1.92*10^{12}$ and $4.06*10^{12}$ years for 320°C, 370°C and 420°C traps respectively, at ambient temperature of 20°C and heating rate of 10°C/s (Han et al., 2000). A lifetime of $1.7*10^7$ years for 325°C trap at ambient temperature 20°C and heating rate 5°C/s (Spooner and Questiaux, 2000). Although, some studies report saturation of TL signals for these dosimetric peaks around 10-40 kGy, but age estimations have not become a reality in this dose range (Durrani et al., 1977;

Sawakuchi and Okuno, 2004; Schmidt and Woda, 2019; Woda et al., 2002). This suggests that attempts to comprehend basic physics and luminescence mechanisms at high radiation doses (HRDs) should be stepped up.

Quartz is known to emit luminescence in several emission bands that are majorly classified as UV, blue, green and red emissions (Götze et al., 2021; Krbetschek et al., 1997; Preusser et al., 2009; Rink et al., 1993). UV emission reaches early saturation around 250 Gy (Adamiec, 2005; Chawla et al., 1998; Wintle, 1997) and shows a supralinear increase thereafter (Chawla et al., 1998). Therefore, it is used for dose estimation below 250 Gy. In blue many studies report very high saturation ~ 40kGy, but no dose estimates at these HRDs are made (Hashimoto et al., 1987; Schmidt and Woda, 2019). Further sensitivity changes are reported in blue TL at HRDs (Hashimoto et al., 1987). Studies using red TL emission from volcanic quartz have obtained saturation dose ~ 6 kGy and are fairly studied for dose estimation (Fattahi and Stokes, 2000; Hashimoto et al., 1987; Miallier et al., 1991). The saturation characteristics for quartz in different emissions, the role of electron traps and recombination centres in saturation is still not understood (Ankjærgaard et al., 2006; Lowick et al., 2010). Therefore, this study attempts a detailed simultaneous analysis of dose saturation across the entire spectral region from UV to red for various HRDs. This will further help in developing an understanding about the associated issues such as defect creations, sensitivity changes, TL peak shifts, emission spectrum changes and possibly help in deconvoluting complex convolution of glow peaks linked with different dose ranges. The study also addresses the effect of normalization, predose (previous dose), bleachability on the TL characteristics at HRDs.

2. METHODOLOGY

2.1. Samples

This study utilizes four quartz samples from different regions of India, details are given in Table 1. YS-5 and SR-23 are fluvial sedimentary sample from Yamuna and Sabarmati basin respectively. A naturally high dose sample KG-1 (in saturation in (SAR-BSL)) from Khari Gorge, Bhuj in Western India was used to study the bleaching effect and natural luminescence in different spectral windows. Apart from these sedimentary samples, a quartzite rock sample RQ-1 from Sabarmati basin was also studied. To confirm the mineralogy of the RQ-1 sample, XRD was carried out, which confirms it to be quartz. Of the four samples used in this study, detailed investigations are carried out on the sample YS-5, because of the less inter-aliquot scatter and clear visibility of saturation of signal.

2.2. Sample preparation

All the samples were processed under subdued red light by first treating them with 1 N HCl to remove carbonates, followed by 30% H_2O_2 to remove organic impurities. A grain size fraction of 90 - 150 µm was dry sieved and magnetically separated using Frantz® magnetic separator (Model LB-1) to separate heavy minerals, quartz and feldspar (Porat, 2006). Cleaned quartz was treated with 40% HF for 60 minutes to remove alpha skin and then with 37% HCl for 30 minutes to remove any fluorides. IR test was done to check feldspar contamination and negligible IR signal was observed (Smith et al., 1990). The rock quartz (RQ-1) sample was obtained by crushing the rock and separating a grain size of 90-150 µm through sieving. This fraction is treated with 10% HF for 5 minutes to remove surface defects formed, if any due to crushing and then by 37% HCl for 30 minutes to remove any fluoride contamination (Toyoda et al., 2000). Monolayer of the sample was mounted on stainless steel disc using Silkospray™ and used for all TL measurements. A sample size of 5 mm was used

on the disc for measurement, thus enabling an average measurement of approximately 2000 grains at a time.

2.3. Instrumentation

Measurements were done in Risø TL/OSL DA-15 automated reader equipped with EMI 9635 QA Photomultiplier tube, Sr^{90}/Y^{90} beta source (dose rate 0.044 Gy/s), and optical head containing Blue and IR LEDs for stimulation (Bøtter-Jensen et al., 2010; Thomsen et al., 2006). A linear heating rate of 2°C/s was employed to heat the samples. A Co-60 gamma source having a dose rate of 0.183 Gy/s in a GC1200 assembly, manufactured indigenously by BRIT (Board of Radiation & Isotope Technology) in India was used for irradiating samples with HRDs >1 kGy. For multi-spectral TL studies, an EMCCD based high sensitivity spectrometer is often required. However, due to the high cost and unavailability of the required instrument, measurements were done using several interference filters as done by many previous studies (Caicedo et al., 2021; Monti et al., 2019; Spooner and Questiaux, 2000). Optical filters used for present study are listed in Table 2 and their spectral transmissions are shown in Fig. 1.

These filters were used in combination with BG39 filter (output from 325 - 700 nm) to reduce IR blackbody background. In addition, suitable neutral density (ND) filters were also used wherever the counts were significantly high and can lead PMT to non-linear region. Osram ultravitalux 300 W solar simulator lamp was used to bleach the samples of previous luminescence signals in addition to natural sunlight whenever needed.

2.4. Measurements

To study the luminescence characteristics for known dose, the signal due to prior dose was removed by bleaching the sediment samples YS-5 and SR-23 in solar lamp for 24 hours. This

reduced the previous TL signals in the samples. As the sensitivity of rock sample (RQ-1) was low and it didn't yield a measurable S/N ratio, it was sensitized by annealing at 450°C for 30 minutes. This removed the previous TL signal and enhanced the dose sensitivity as well as stabilizing it. Following this, the samples were irradiated with known doses. Apart from KG-1 (as it was already in saturation in SAR-BSL), all samples were irradiated with gamma radiation from 1 to 21 kGy. The following experiments are conducted.

2.4.1. Trap Characterization

It has been reported that quartz has several traps (Aitken, 1985; Khoury et al., 2008). Hence a T_{max}-T_{stop} analysis was carried out (Garlick and Gibson, 1948; McKeever, 1985; Pagonis et al., 2006). The sample was irradiated with a dose of 50 Gy, and preheated till T_{stop} (from 30 to 450°C, in steps of 10°C) followed by a measurement of TL 450°C. To avoid irradiation of samples multiple times (as is done in T_{max}-$T_{stop)}$, the activation energy (E_a) was estimated using the repeated initial rise method (fractional glow technique) (Gobrecht and Hofmann, 1966), thus enabling the study of trap characteristics at HRDs. This method enables the determination of E_a of trap of any order. The initial part of the glow curve was analysed which is known to follow first-order kinetics. The method here was applied on 50 Gy, 3000 Gy and 18000 Gy dosed samples. The irradiated samples were heated till T_{stop} (from 30 to 450°C, in steps of 5°C), cooled and heated again. The blackbody subtracted intensity was used to compute the activation energy using Arrhenius relation between intensity and temperature (Pagonis et al., 2006). Additionally, to observe the effect of HRD on trap characteristics after annealing, a dose of 50 Gy was administered and activation energy was re-estimated.

2.4.2. Thermoluminescence glow curves and dose response

The TL glow curves of all the samples were measured for variable doses in the range 1-21 kGy in spectrum range (325-700 nm) using a BG39 filter. A preheat of 260°C for 10 s was used to remove the contribution from shallow traps, which generally overpowers the signal from higher temperature peaks (>300°C) (Spooner and Questiaux, 2000). Multiple aliquot additive dose (MAAD) response curves were obtained using mass normalized integrated TL intensity in 340-380°C temperature range. The MAAD protocol ensures the measurement of samples at similar sensitivity. Three aliquots were measured for each dose point. For samples SR-23 and YS-5, a test dose of 21 Gy was added to measure low-temperature peak 80-100°C TL peak for using it to monitor zero glow sensitivity. The saturation dose was found by fitting a single saturating exponential equation, $I = I_0\left(1 - e^{-D/D_0}\right)$, where I_0 is the saturation intensity and D_0 is the characteristics dose (Murray and Wintle, 2000). The maximum dose (saturation dose) that can be estimated is $2D_0$ which corresponds to 86% of the maximum intensity is calculated (Wintle and Murray, 2006). Additionally, a preheat of 350°C was used based on T_{max}-T_{stop} analysis to remove shallower traps in the region 300-400°C and $2D_0$ was calculated.

2.4.3. Multi-spectral studies

Multi-spectral studies were carried out using various bandpass filters (details in Table 2). The variation of TL response in different emission bands was studied for the sample YS-5 for an irradiation dose of 1 kGy and a test dose of 21 Gy (zero glow) by heating linearly up to 450°C at a rate of 2°C/s. Following this, the dose response curve (DRC) is obtained for HRD as per section 2.4.2. in various spectral regions and $2D_0$ was estimated.

2.4.4. Signal resetting by sunlight

For dating applications, an important requirement for any signal is its resetting before burial by sunlight or heat or the reduction of signal to residual level before burial. The TL dating method can be applied to sunlight resettable events by subtracting the residual dose found by laboratory experiments (Singhvi and Mejdahl, 1985). Thus, bleachability of different TL spectral bands by sunlight and the magnitude of the residuals was investigated. The aliquots of naturally irradiated quartz sample KG-1 were exposed to sunlight for different time periods of 30 s, 1 min, 10 min, 30 min, 1 hour, 2 hour and 3 hour. Their respective TL responses were measured following sunlight exposure.

2.4.5. Sensitivity normalization

For inter-aliquot comparisons proper normalization of signal corresponding to a given dose is required. It may include normalization by mass, which assumes homogeneity in luminescence sensitivity of the grains throughout the sample, or by luminescence response of same or another peak, which assumes the signal to be proportional to mass and also takes care of fluctuations during measurements. These methods are well tested and characterized for low doses, but needs to be verified for HRDs. Hence, the zero glow and second glow normalized signal corresponding to a test dose of 21Gy were compared with mass normalized signal as per protocol given in Table 3. The zero glow normalization was obtained by dividing the integrated TL1 signal intensity in the range 340-380°C with the integrated TL1 intensity in the range of 80-100°C. Similarly, in the second glow normalization the integrated TL1 intensity in range 340-380°C is normalized with the integrated TL2 intensity in range 80-100°C, obtained after test dose TD2.

2.4.6. High radiation predose (HRpD) effect

Effect of HRpDs on the TL signals of the samples was studied. For this, the TL intensity of various trapping and recombination centres was examined. Fresh samples were divided into 8

batches and each batch was given a different dose in range 1-21 kGy followed by TL wash up to 450°C to remove signal stored due to this dose. Then an identical dose was given to all batches followed by TL measurement (Table 4). The measurements were made in various wavelengths to see the characteristics of various recombination centres.

3. RESULTS

3.1. Trap characteristics

The TL glow curves of sample YS-5 measured following varying preheat temperatures are shown in Fig. 2. Several traps are observed and are marked with black arrows. It shows that at least three traps are present beyond 300°C. Further, Fig. 3 shows the T_{max}- T_{stop} graph for the sample YS-5. Multiple traps are visible for temperatures <200°C and a continuum in T_{stop} is observed for temperatures > 200°C and T_{max} is found to increase towards end. The activation energy estimated at various doses is shown in Fig. 4(a), the curve for 50 Gy shows multiple plateaus, in agreement with the multiple traps observed in TL glow curve (Fig. 2). Towards the end the errors increase, because of poor signal to noise (S/N) ratio. However, at 3 kGy and 18 kGy significant differences in the activation energy of the quartz system are observed at low (< 200°C) temperatures and small variations at high (> 350°C) temperatures. The 110°C peak has a low lifetime (~8 hrs) (Aitken, 1985). The time of gamma irradiation of samples with 3 and 18 kGy and time of transportation of samples is significantly higher than lifetime of low-temperature peak leading to thermal fading, hence activation energy for this peak for HRDs could not be calculated. Further, for HRDs, the activation energy distribution for higher temperatures becomes like a continuum, rather than plateaus that are observed at 50 Gy. Further Fig. 4(b) shows the comparison of activation energies for 50 Gy doses before

and after different HRD treatment of samples. Results shows that the E_a attempts to restore once the high doses are removed.

3.2. Dose Response Characteristics

Fig. 5(a), S2(a) and S3(a) represent the TL glow curves of the quartz samples (YS-5, RQ-1 and SR-23) for increasing HRDs. The TL peak intensity increases with HRD maintaining the glow curve shapes throughout the temperature range. Insets of Fig. 5(a) and S3(a) show the 110°C zero glow peak response to a dose of 21 Gy, appearing around 90°C in these experiments. Such a shift in the peak has previously been reported (theoretically and experimentally) and is due to changes in heating rate (Pagonis et al., 2006). At a heating rate of 2°C/s it appears at 90°C, but at 5°C/s, it is at 110°C (see supplementary Fig. S1). For the sample YS-5, dose quenching (Bailiff, 1994; Oniya, 2014) in the low-temperature (80-100°C) peak is observed with the increase in the HRD Fig. 5(a), inset. However, no quenching is observed for the sample SR-23, Fig. S3(a) inset. Fig. 5(b), S2(b), and S3(b) show the DRC for 340-380°C peak. The saturation dose ($2D_0$) that can be estimated is ~18 kGy in the annealed rock quartz sample (RQ-1), and 8.12 ± 1.8 kGy and 11 ± 1 kGy for the sedimentary samples, SR-23 and YS-5 respectively. In the initial part of the DRC of sample RQ-1, supralinearity is observed with an increase in dose. This changed to linear characteristics after 6 kGy, and to sublinearity after 15 kGy. Fig. 6 shows the DRC comparison for a preheat temperature of 260°C and 350°C and the $2D_0$ is 9.2 ± 1.3 and 13.3 ± 1 kGy respectively. The saturation dose is found to increase by 40% in the case when higher preheat is used.

A slight shift in peak maxima is observed in all the glow curves towards higher temperatures with an increase in dose. The extent of peak shift is measured from the TL glow curves by

noting the temperature corresponding to maximum intensity in the >300°C temperature region. With increase in dose, the peak maximum shifts towards higher temperature by 35°C from 1 to 15 kGy for sample RQ-1, 25°C from 1 to 12 kGy dose for the sample YS-5, after which signal saturates and no further shift in peak maximum is observed. However, for the sample SR-23, peak temperature first decreases by 10°C from 1 to 3 kGy, then it increases by 15 °C till 12 kGy.

3.3. Multi-spectral emission studies

Fig. 7 shows the glow curves for sample YS-5 irradiated with 1 kGy dose in different emission bands (Table 2). The low-temperature peak is most prominent in UV emission for 21 Gy dose after a TL 450°C wash (supplementary, Fig. S4). It is observed that the high-temperature peak (>300°C) has emissions in all selected spectral bands. However, the relative intensity of low-temperature peak w.r.t. high-temperature peak varies. The ratio is lower for higher wavelengths and maximum for the UV emission (340± 40 nm). The DRC in red and UV are shown in Fig. 8 (rest in supplementary Fig. S5). All the DRCs have $2D_0$ within 2σ (Grey Band) of the mean 11 kGy as shown in Fig. 9. DRC for all emissions for annealed RQ-1 are shown in supplementary, Fig. S6. It shows a similar linear increase with dose in all emissions and no saturation is observed.

3.4. Signal resetting by sunlight

Fig. 10 shows the effect of sunlight exposure on TL intensity of the sample KG-1, in various spectral regions. The mass normalized TL signal of bleached aliquot is further normalized by the mass normalized counts of non-exposed aliquot. The red emission counts in present setup are an order less than other emissions, thus has larger error. The high-temperature region is further divided into two regions with 320-330°C and 370-380°C, integrated mass normalized counts in these regions are plotted in supplementary, Fig. S7. The bleachability of the region

370-380°C is less than 320-330°C. Further, it is found to decrease with increasing emission wavelength. The red signal is found to be the least bleachable for both regions.

3.5. Sensitivity normalization

Fig. 11 shows the comparison of DRC for signal normalized by mass, zero glow and second glow for the sample YS-5 in visible emission (325-700 nm). Normalization results for specific emission bands are shown in Fig. S8. The $2D_0$ of 11 ± 1 kGy, 143 ± 55 kGy, 19.6 ± 2.6 kGy for mass normalization, zero glow normalization and second glow normalization are obtained respectively. Zero glow normalization shows linear increase with dose and no saturation is observed. Such huge differences implicate caution during normalization.

3.6. High radiation predose

The results for HRpD experiment (Table 4) on sample RQ-1 are shown in Fig. 12(a) and 12(b). The 340-380°C peak intensity for a 34 Gy test dose is dependent on the HRpD. This dependence is observed in all emission bands. For low doses, intensity first increases with previous dose and then saturates after 10 kGy dose. Similarly, for the low-temperature peak, the intensity for the same 34 Gy test dose is dependent on the previous dose except for the blue emission. The low-temperature UV emission, sensitivity decreases with increase in HRpD and around 10 kGy becomes constant. For low-temperature 447 and 475 nm emission bands, sensitivity has negligible dependence on HRpD. However, for 520, 550 and 620 nm emission, low-temperature peak intensity increases with HRpD.

4. DISCUSSION

Till date, the use of quartz for dosimetry and dating is limited to a dose of ~250 Gy (Chawla et al., 1998; Fleming, 1969; Huntley et al., 1996) using conventional UV (340 nm) emission. The lack of understanding of quartz luminescence characteristics at HRD limits the

application for HRD estimation. The results obtained provide new insights about the luminescence phenomenon at HRD as discussed below.

4.1. Dose response and trap characteristics

The DRCs measured in visible region using BG39 bandpass filter for HRDs indicate that saturation dose is about 50 - 100 times higher (~10-18 kGy) (Fig. 5, S2 and S3) than conventional methods, which implicates potential to increase the dating limit by two order of magnitude. This result is in agreement with previous studies (Durrani et al., 1977; Kuhn et al., 2000; Ogundare et al., 2006; Sawakuchi and Okuno, 2004; Schmidt and Woda, 2019; Woda et al., 2002). Additionally, the DRCs show saturation (Fig. S3 and 5) of signal which is unexpected if new defects centres are created during HRD. In such cases, defect creation should be a continuous process and saturation should not be observed. The damage to crystal structure can be associated with unpredictable luminescence behaviour instead of monotonous increase towards saturation with increasing dose (Hegde et al., 2019).

Trap kinetic parameters such as τ, E_a and s also gives insights into the trap structure with the changing HRDs. Fig. 4 shows the activation energy (E_a) estimated for different radiation doses. Results show that low-temperature traps (< 200°C) are majorly affected during HRDs as their activation energy increases. This signifies that the potential energy at the site of these electronic states is modified due to accumulation of large trapped charges. Higher activation energy indicates towards lesser probability of eviction at room temperature and strongly bound charges, which are difficult to evict. However, the deeper traps at temperatures > 200°C are much more stable in terms of changes in activation energy, with HRD. This is in agreement with study by Hunter et al., (2018) on the blue emission for 210°C and 350°C peaks, which show that the kinetic parameters remain unaltered at HRDs. Annealing samples

by heating to 450°C reduces the activation energy of the low-temperature traps (Fig. 4(b)). This again indicates that permanent defect creation does not occur due to HRD and after removal of charges from trapping centre, crystal attempts to restore the original configuration of traps in crystal.

4.2. Peak shift with dose

Fig. 5(a), S2(a) and S3(a) shows a shift in the TL peak maximum temperature towards higher temperature with increase in dose. McKeever, (1985) suggested that for non-first order kinetics TL glow peak temperature shifts to lower temperatures with increase in dose as observed for high-temperature (250-450°C) TL peak at 3kGy for the sample SR-23 (Fig. S3(a)). However, for doses > 3 kGy, the peak maximum for high-temperature (250-450°C) TL peak shifts to higher temperatures with dose. Similarly, a shift in peak maximum to higher temperature is observed for the samples RQ-1 and YS-5 (Fig. S2(a) and 5(a)) for the high-temperature (250-450°C) TL peak. Such a shift can be explained based on the variable electron capture cross-sections of different traps, resulting in different saturation (suggested by Ogundare et al., (2006)). Fig. 2 suggests that there are multiple traps contributing to TL signal in quartz above 300°C. Traps beyond 200°C could not be distinguished in Fig. 3 because of the overpowering intensity from 350°C peak. For deep traps having peak temperature > 350°C the saturation dose is significantly higher (Fig. 6). Presence of multiple traps with different saturation characteristics, results in continuous increase in intensity of deeper traps even after comparatively shallow traps are saturated resulting in shift of peak maxima towards higher temperature. Durrani et al., (1977) have reported that the saturation dose of all traps at HRDs in quartz is similar ~ 20 kGy. However, due to the low dose resolution in their study, it was difficult to observe changes in saturation of different traps. Schmidt and Woda, (2019) have also reported on the shifting of blue TL peak maximum to

higher temperature with increase in doses which is consistent with the results of present study.

4.3. Multi-Spectral Studies

Quartz TL is complex in nature, consisting of several traps and recombination centres or emissions. The luminescence spectral characteristics measured using different filter combinations spanning the full transmission range from UV to red (300-660 nm) are shown in Fig. 7-10 and Fig. 12.

Fig. 7 shows TL glow curves of quartz in various emission wavelengths ranging from UV to red for sample YS-5. Similarly, TL glow curves were also measured for all samples in the mentioned bands. With the increase in HRD from 1 to 21 kGy, increase in the signal intensity in all emissions is observed (Fig. 8, S5, S6). This is different from the observation mentioned by Schmidt and Woda, (2019) that with increase in dose to kGy level some emissions in quartz become diminished while blue emissions dominate.

Fig. 8 and 9 shows that the saturation dose ($2D_0$) is similar for all emissions within 2 sigma of the mean. This possibly suggests that for measured samples, the recombination centres may not have any role in dose saturation and it is mainly controlled by the charge population of the trapping centre. Possibly, there is an excess of recombination centres, thus sufficient numbers are available for all the emission bands. Similar estimates are made by other researchers like, the saturation dose for red TL agrees with our results (Miallier et al., 1991; Westaway and Roberts, 2006). Some works also report an increase in TL intensity in blue up to ~10 kGy (Hashimoto et al., 1987; Hunter et al., 2018; Schmidt and Woda, 2019). Study by Lowick et al., (2010) on TL also shows an increasing luminescence emission in both blue and UV until 1.2 kGy, although they didn't record for higher doses. Besides this, study using the

optically and thermally stimulated electrons (OSE and TSE) (Ankjærgaard et al., 2006) have shown that trapping centres in quartz do not saturate till 10 kGy and may even go beyond that. Collectively, the results of present study agree with these previous results.

4.4. Signal Resetting

It is observed that bleachability of 320-330°C TL peak region is better than 370-380°C region (Fig. S7) for all emissions and accords with earlier observations (Wintle, 1997). It is seen that for higher emission wavelengths, the bleachability is low (Fig. 10, S7). The UV emissions has the least residuals (most bleachable) and red has the maximum residual (least bleachable). Although it appears to be linked to recombination centre, the exact mechanism is not yet clear and need more investigation. One of the possibilities could be that the charges in the recombination centres associated with higher wavelength emission (i.e., red emission) are tightly bound and are thus slow to bleach, however more detailed investigations are needed. The results are consistent with the previous findings on blue, UV TL (Singhvi et al., 1982) and red TL (Lai and Murray, 2006; Miallier et al., 1994). This indicates that the role of recombination centres is overlooked and needs more attention.

4.5. Normalization, Dose Quenching

Ideally for adequate normalization, the observed dose signal and corresponding test dose signal should have identical sensitivity changes with the measurement cycle and dose. It is expected that the saturation dose should be independent of normalization method and various normalization methods should give identical saturation dose. Fig. 11, shows that saturation characteristics of different normalization methods does not match. Here, the mass normalization is taken as standard normalization for reference, as it is not influenced by any other signal characteristics. The deviations of zero glow and second glow normalization suggest that low-temperature peak and 340-380°C peak does not respond to dose in similar

way. The increase in the zero glow normalized signal intensity beyond mass normalized intensity in the Fig. 11 is due to decrease in the low-temperature peak intensity with dose as shown in Fig. 5(b) resulting from quenching of signal during high dose irradiation (Bailiff, 1994; Oniya, 2014). The trap competition can significantly influence the normalization process. During zero glow normalization irradiation fills charges in traps 80-100°C peak when high-temperature peaks (340-380°C) are already filled, whereas for second glow normalization, irradiation fills 80-100°C traps while high-temperature traps (340-380°C) are empty. However, as evident from Fig. 4(b), the low-temperature trap system (<200°C) attempts to restore after HRD but does not exactly match the original trap system; differences in the saturation of mass and second glow normalized DRC are observed. Thus choice of normalization technique at HRDs is crucial. In the present case mass normalization is found to provide better results as shown in Fig. 11 as it is unaffected by the intrinsic characteristics traps and more suitable to normalize inter-aliquot variations.

4.6. High Radiation Predose (HRpD) effects

Fig. 12 (a) shows that 110°C TL sensitivity in different emissions is drastically affected by the HRpD. Different emission centres are affected differently. The UV emissions are quenched by HRpD, while blue is unaffected (in comparison to other) and green and red are enhanced. For the 340-380°C TL, all centres signal is enhanced, but to different extents. The enhancement is greatest in yellow-green (550 nm), followed by green (520 nm) and blue (447 and 475 nm). HRpD effects have been observed in several studies (Oniya, 2014; Stoneham and Stokes, 1991; Zimmerman, 1971). However, the majority of these studies are done in the ultraviolet or blue luminescence emissions. The decreased response of low-temperature TL peak emission in the ultraviolet region (290-390 nm) is in agreement with observation of Jain et al., (2003). Further, the study by Hunter et al., (2018) shows sensitization of high-

temperature peak (350°C) by HRpD similar to current observations. Woda et al., (2002) have shown that different EPR centres in quartz respond differently to HRpD e.g. the Ge-Li and Ge-Na centre first increases with dose than decreases, whereas, the Al centre continuously increases. However, there have always been ambiguity on the matter that which centre corresponds to which emission. The results further signify the importance of recombination centres in the luminescence response. The enhancement in the sensitivity of 340-380°C TL intensity and the lack of correlated enhanced signal for test dose, restricts us to use single aliquot regenerative type protocols to estimate doses for HRD. However, since the DRC shows dose response till ~10 kGy and ~18 kGy (annealed rock quartz), dose estimation for HRD should be advanced with additive approach.

5. CONCLUSIONS

Present work investigated quartz samples from different provenance at high radiation doses (1-21 kGy), for several properties like dose-response, trap characteristics, bleachability, normalization and predose effects. Quartz has the potential to estimate doses 50-100 times the present limit. The work enhances the role of recombination centres in the luminescence mechanism.

This study leads to the following major conclusion

1. Activation energy for the traps present at temperature < 200°C, increases at HRDs. Further after removal of high dose, the activation energy decreases and approaches the low dose values.
2. TL signal in 340-380°C temperature range of quartz increase with doses up to 18 kGy for annealed rock quartz and around 11 kGy for sedimentary quartz in the spectral range of 325-700 nm.

3. The spectral analysis of the luminescence emission signifies that the trapping centres are majorly responsible for saturation in the samples and the saturation dose is similar within error for all emissions wavelengths from UV to red.
4. The TL signal (340-380°C) is bleachable by sunlight. The bleachability is found to be anticorrelated with emission wavelength and the mechanism needs further investigation.
5. Zero glow and second glow normalization are not appropriate for sensitivity correction at HRDs and mass normalization should be used.
6. HRpD enhances the signal intensity of all emissions in the 340-380°C temperature range and green and red 80-100°C emissions, while there is a quenching of the UV 80-100°C and blue 80-100°C is independent in comparison to others.

Supplementary material

See supplementary material for detailed glow curves and DRC in different emissions.

Data availability

Data will be made available on request.

Acknowledgement

The authors would like to thank Dr. Munish Ksumar, BARC for help with gamma irradiation of samples and discussion on the manuscript, Dr. V. Sathian, Head, RSS, RSSD, BARC, Smt. M. Menaka, Head, RAMS, IGCAR and Dr. Balasubramanian Venkatraman, director IGCAR for providing high-dose irradiation facility. The work carried out at PRL is supported by the Department of Space, Government of India.

Author Declarations

Conflict of interest

459 The authors have no conflicts to disclose.

460 Author contributions

461 **Malika Singhal:** Conceptualization; Data curation; Formal analysis; Investigation;
462 Methodology; Discussion; Writing – original draft. **Madhusmita Panda:** Data curation;
463 Methodology; Writing – review & editing. **S. H. Shinde:** Methodology; Writing – review &
464 editing. **Sandip Mondal:** Methodology; Writing – review & editing. **O. Annalakshmi:** Data
465 curation; Methodology; Discussion; Writing – review & editing. **Naveen Chauhan:**
466 Conceptualization; Formal analysis; Investigation; Methodology; Resources; Supervision;
467 Discussion; Writing – review & editing.

468

469 **References**

470 Adamiec, G., 2005. Properties of the 360 and 550nm TL emissions of the '110° C peak'in
471 fired quartz. Radiat. Meas. 39, 105–110.

472 Aitken, M.J., 1985. Thermoluminescence Dating, Handbooks for archaeologists : a
473 publication of the sub-committee for archaeology of the standing committee for the
474 humanities. Academic Press.

475 Ankjærgaard, C., Guralnik, B., Buylaert, J.P., Reimann, T., Yi, S.W., Wallinga, J., 2016.
476 Violet stimulated luminescence dating of quartz from Luochuan (Chinese loess plateau):
477 Agreement with independent chronology up to ~600 ka. Quat. Geochronol. 34, 33–46.
478 https://doi.org/10.1016/j.quageo.2016.03.001

479 Ankjærgaard, C., Murray, A.S., Denby, P.M., Z, L.B., 2006. Measurement of optically and
480 thermally stimulated electron emission from natural minerals 41, 780–786.
481 https://doi.org/10.1016/j.radmeas.2006.05.012

482 Bailiff, I.K., 1994. The pre-dose technique. Radiat. Meas. 23, 471–479.

483 Bøtter-Jensen, L., Thomsen, K.J., Jain, M., 2010. Review of optically stimulated
484 luminescence (OSL) instrumental developments for retrospective dosimetry. Radiat.
485 Meas. 45, 253–257. https://doi.org/https://doi.org/10.1016/j.radmeas.2009.11.030

Buylaert, J.P., Thiel, C., Murray, A.S., Vandenberghe, D.A.G., Yi, S., Lu, H., 2011. Irsl and post-ir irsl residual doses recorded in modern dust samples from the chinese loess plateau. Geochronometria 38, 432–440. https://doi.org/10.2478/s13386-011-0047-0

Caicedo, F.D., Asfora, V.K., Guzzo, P.L., Barros, V.S.M., 2021. Nuclear Inst . and Methods in Physics Research , B Investigation of the spectrally resolved TL signals of natural quartz single crystals sensitized by high-dose of gamma-radiation and moderate. Nucl. Inst. Methods Phys. Res. B 486, 37–47. https://doi.org/10.1016/j.nimb.2020.11.001

Chawla, S., Gundu Rao, T.K., Singhvi, A.K., 1998. Quartz thermoluminescence: Dose and dose-rate effects and their implications. Radiat. Meas. 29, 53–63. https://doi.org/10.1016/S1350-4487(97)00200-X

Duller, G.A.T., Wintle, A.G., 2012. A review of the thermally transferred optically stimulated luminescence signal from quartz for dating sediments. Quat. Geochronol. 7, 6–20. https://doi.org/10.1016/j.quageo.2011.09.003

Durrani, S.A., Khazal, K.A.R., McKeever, S.W.S., Riley, R.J., 1977. Studies of changes in the thermoluminescence sensitivity in quartz induced by proton and gamma irradiations. Radiat. Eff. 33, 237–244. https://doi.org/10.1080/00337577708233112

Fattahi, M., Stokes, S., 2003. Dating volcanic and related sediments by luminescence methods: A review. Earth-Science Rev. 62, 229–264. https://doi.org/10.1016/S0012-8252(02)00159-9

Fattahi, M., Stokes, S., 2000. Extending the time range of luminescence dating using red TL (RTL) from volcanic quartz. Radiat. Meas. 32, 479–485. https://doi.org/10.1016/S1350-4487(00)00105-0

Fleming, S., 1969. The acquisition of radiothermoluminescence by ancient ceramics. D.Phil thesis, Oxford University.

Garlick, G.F.J., Gibson, A.F., 1948. The electron trap mechanism of luminescence in sulphide and silicate phosphors. Proc. Phys. Soc. 60, 574.

Gobrecht, H., Hofmann, D., 1966. Spectroscopy of traps by fractional glow technique. J.

513 Phys. Chem. Solids 27, 509–522.

514 Götze, J., Pan, Y., Müller, A., 2021. Mineralogy and mineral chemistry of quartz: A review.
515 Mineral. Mag. 85, 639–664. https://doi.org/10.1180/mgm.2021.72

516 Han, Z.-Y., Li, S.-H., Tso, M.-Y.W., 2000. Lifetime estimation of thermoluminescence traps
517 in granitic quartz. Radiat. Eff. defects solids 152, 307–314.

518 Hashimoto, T., Yokosaka, K., Habuki, H., 1987. Emission properties of thermoluminescence
519 from natural quartz-blue and red TL response to absorbed dose. Int. J. Radiat. Appl.
520 Instrumentation. Part 13, 57–66. https://doi.org/10.1016/1359-0189(87)90008-2

521 Hegde, V., Chauhan, N., Kumar, V., Viswanath, C.S.D., Mahato, K.K., Kamath, S.D., 2019.
522 Effects of high dose gamma irradiation on the optical properties of Eu3+ doped zinc
523 sodium bismuth borate glasses for red LEDs. J. Lumin. 207, 288–300.
524 https://doi.org/10.1016/j.jlumin.2018.11.023

525 Hunter, P.G., Spooner, N.A., Smith, B.W., 2018. Thermoluminescence emission from quartz
526 at 480 nm as a high-dose radiation marker. Radiat. Meas. 120, 143–147.
527 https://doi.org/10.1016/j.radmeas.2018.04.001

528 Huntley, D.J., Short, M.A., Dunphy, K., 1996. Deep traps in quartz and their use for optical
529 dating. Can. J. Phys. 74, 81–91.

530 Jain, M., 2009. Extending the dose range: Probing deep traps in quartz with 3.06 eV photons.
531 Radiat. Meas. 44, 445–452. https://doi.org/10.1016/j.radmeas.2009.03.011

532 Jain, M., Bøtter-Jensen, L., Singhvi, A.K., 2003. Dose evaluation using multiple-aliquot
533 quartz OSL: Test of methods and a new protocol for improved accuracy and precision.
534 Radiat. Meas. 37, 67–80. https://doi.org/10.1016/S1350-4487(02)00165-8

535 Kars, R.H., Wallinga, J., Cohen, K.M., 2008. A new approach towards anomalous fading
536 correction for feldspar IRSL dating - tests on samples in field saturation. Radiat. Meas.
537 43, 786–790. https://doi.org/10.1016/j.radmeas.2008.01.021

538 Khoury, H.J., Guzzo, P.L., Souza, L.B.F., Farias, T.M.B., Watanabe, S., 2008. TL dosimetry

of natural quartz sensitized by heat-treatment and high dose irradiation 43, 487–491. https://doi.org/10.1016/j.radmeas.2008.01.028

Krbetschek, M.R., Götze, J., Dietrich, A., Trautmann, T., 1997. Spectral information from minerals relevant for luminescence dating. Radiat. Meas. 27, 695–748. https://doi.org/10.1016/S1350-4487(97)00223-0

Kuhn, R., Trautmann, T., Singhvi, A.K., Krbetschek, M.R., Wagner, G.A., Stolz, W., 2000. Study of thermoluminescence emission spectra and optical stimulation spectra of quartz from different provenances. Radiat. Meas. 32, 653–657. https://doi.org/10.1016/S1350-4487(00)00090-1

Lai, Z., Murray, A., 2006. Red TL of quartz extracted from Chinese loess : Bleachability and saturation dose 41, 836–840. https://doi.org/10.1016/j.radmeas.2006.04.017

Lowick, S.E., Preusser, F., Wintle, A.G., 2010. Investigating quartz optically stimulated luminescence dose-response curves at high doses. Radiat. Meas. 45, 975–984. https://doi.org/10.1016/j.radmeas.2010.07.010

McKeever, S.W.S., 1985. Thermoluminescence of solids. Cambridge University Press.

Miallier, D., Fain, J., Montret, M., Pilleyre, T., Sanzelle, S., Soumana, S., 1994. Sun bleaching of the red TL of quartz: preliminary observations. Anc. TL 12, 1–4.

Miallier, D., Fain, J., Montret, M., Pilleyre, T., Sanzelle, S., Soumana, S., 1991. Properties of the red TL peak of quartz relevant to thermoluminescence dating. Int. J. Radiat. Appl. Instrumentation. Part D. Nucl. Tracks Radiat. Meas. 18, 89–94.

Monti, A.M., Fasoli, M., Panzeri, L., Martini, M., 2019. Investigation of the spectrally resolved TL peaks of quartz in the 70°C–220°C temperature region. Radiat. Meas. 127, 106141. https://doi.org/10.1016/j.radmeas.2019.106141

Murray, A., Arnold, L.J., Buylaert, J.-P., Guérin, G., Qin, J., Singhvi, A.K., Smedley, R., Thomsen, K.J., 2021. Optically stimulated luminescence dating using quartz, Nature Reviews Methods Primers. https://doi.org/10.1038/s43586-021-00068-5

565 Murray, A.S., Wintle, A.G., 2000. Luminescence dating of quartz using an improved single-
566 aliquot regenerative-dose protocol. Radiat. Meas. 32, 57–73.
567 https://doi.org/10.1016/S1350-4487(99)00253-X

568 Ogundare, F.O., Chithambo, M.L., Oniya, E.O., 2006. Anomalous behaviour of
569 thermoluminescence from quartz: A case of glow peaks from a Nigerian quartz. Radiat.
570 Meas. 41, 549–553. https://doi.org/10.1016/j.radmeas.2006.03.001

571 Oniya, E.O., 2014. Luminescence Sensitisation of Natural Quartz Using Pre-Exposure Dose
572 and Thermal Activation Techniques. Ph.D. thesis, University of Ibadan.

573 Pagonis, V., Kitis, G., Furetta, C., 2006. Numerical and practical exercises in
574 thermoluminescence, Numerical and Practical Exercises in Thermoluminescence.
575 https://doi.org/10.1007/0-387-30090-2

576 Porat, N., 2006. Use of magnetic separation for purifying quartz for luminescence dating.
577 Anc. TL 24, 33–36.

578 Preusser, F., Chithambo, M.L., Götte, T., Martini, M., Ramseyer, K., Sendezera, E.J., Susino,
579 G.J., Wintle, A.G., 2009. Quartz as a natural luminescence dosimeter. Earth-Science
580 Rev. 97, 184–214. https://doi.org/10.1016/j.earscirev.2009.09.006

581 Rink, W.J., Rendell, H., Marseglia, E.A., Luff, B.J., Townsend, P.D., 1993.
582 Thermoluminescence spectra of igneous quartz and hydrothermal vein quartz. Phys.
583 Chem. Miner. 20, 353–361. https://doi.org/10.1007/BF00215106

584 Sawakuchi, G.O., Okuno, E., 2004. Effects of high gamma ray doses in quartz. Nucl.
585 Instruments Methods Phys. Res. Sect. B Beam Interact. with Mater. Atoms 218, 217–
586 221. https://doi.org/10.1016/j.nimb.2003.12.021

587 Schmidt, C., Woda, C., 2019. Quartz thermoluminescence spectra in the high-dose range.
588 Phys. Chem. Miner. 46, 861–875. https://doi.org/10.1007/s00269-019-01046-w

589 Singhvi, A.K., Mejdahl, V., 1985. Thermoluminescence dating of sediments. Nucl. Tracks
590 Radiat. Meas. 10, 137–161.

591 Singhvi, A.K., Sharma, Y.P., Agrawal, D.P., 1982. Thermoluminescence dating of sand
592 dunes in Rajasthan, IND. Nature 295, 313–315. https://doi.org/10.1038/295313a0

593 Smith, B.W., Rhodes, E.J., Stokes, S., Spooner, N.A., Aitken, M.J., 1990. Optical dating of
594 sediments: initial quartz results from Oxford. Archaeometry 32, 19–31.

595 Spooner, N.A., Questiaux, D.G., 2000. Kinetics of red, blue and UV thermoluminescence and
596 optically-stimulated luminescence from quartz. Radiat. Meas. 32, 659–666.
597 https://doi.org/10.1016/S1350-4487(00)00067-6

598 Stoneham, D., Stokes, S., 1991. An investigation of the relationship between the 110° C TL
599 peak and optically stimulated luminescence in sedimentary quartz. Int. J. Radiat. Appl.
600 Instrumentation. Part D. Nucl. Tracks Radiat. Meas. 18, 119–123.

601 Thiel, C., Buylaert, J.P., Murray, A., Terhorst, B., Hofer, I., Tsukamoto, S., Frechen, M.,
602 2011. Luminescence dating of the Stratzing loess profile (Austria) - Testing the potential
603 of an elevated temperature post-IR IRSL protocol. Quat. Int. 234, 23–31.
604 https://doi.org/10.1016/j.quaint.2010.05.018

605 Thomsen, K.J., Bøtter-Jensen, L., Denby, P.M., Moska, P., Murray, A.S., 2006.
606 Developments in luminescence measurement techniques. Radiat. Meas. 41, 768–773.
607 https://doi.org/10.1016/j.radmeas.2006.06.010

608 Toyoda, S., Rink, W.J., Schwarcz, H.P., Rees-Jones, J., 2000. Crushing effects on TL and
609 OSL on quartz: relevance to fault dating. Radiat. Meas. 32, 667–672.

610 Wang, X.L., Lu, Y.C., Wintle, A.G., 2006. Recuperated OSL dating of fine-grained quartz in
611 Chinese loess. Quat. Geochronol. 1, 89–100.
612 https://doi.org/10.1016/j.quageo.2006.05.020

613 Westaway, K.E., Roberts, R.G., 2006. A dual-aliquot regenerative-dose protocol (DAP) for
614 thermoluminescence (TL) dating of quartz sediments using the light-sensitive and
615 isothermally stimulated red emissions. Quat. Sci. Rev. 25, 2513–2528.
616 https://doi.org/10.1016/j.quascirev.2005.06.010

617 Wintle, A.G., 1997. Luminescence dating: Laboratory procedures and protocols. Radiat.

618 Meas. 27, 769–817. https://doi.org/10.1016/S1350-4487(97)00220-5

619 Wintle, A.G., Murray, A.S., 2006. A review of quartz optically stimulated luminescence
620 characteristics and their relevance in single-aliquot regeneration dating protocols.
621 Radiat. Meas. 41, 369–391. https://doi.org/10.1016/j.radmeas.2005.11.001

622 Woda, C., Schilles, T., Rieser, U., Mangini, A., Wagner, G.A., 2002. Point defects and the
623 blue emission in fired quartz at high doses: A comparative luminescence and EPR study
624 100, 261–264.

625 Zimmerman, J., 1971. The radiation-induced increase of the 100 C thermoluminescence
626 sensitivity of fired quartz. J. Phys. C Solid State Phys. 4, 3265–3276.
627 https://doi.org/10.1088/0022-3719/4/18/032

628

629 **Tables:**

630 Table 1: Sample details

Sl. No.	Sample Name	Provenance	Latitude	Longitude
1	YS-5	Yamuna Basin	29°45'47.80"N	77° 8' 29.20"E
2	SR-23	Sabarmati Basin	24°29'12.00"N	73°13' 18.00"E
3	KG-1	Khari Gorge, Bhuj	23° 15' 3.24" N	69° 37' 48.72" E
4	RQ-1	Sabarmati Basin	24°29'12.00"N	73°13'18.00"E

631

632

633 Table 2: Specification of different optical filters used in the study.

Filter Name	Central wavelength (nm)	Bandwidth (nm)
UV_{340}	340	80
$Blue_{447}$	447	60
$Blue_{475}$	475	50
$Green_{520}$	520	70
$Yellow_{550}$	550	100
Red_{620}	620	60

634

635

636 Table 3: Protocol to study various normalization method.

Step no.	Operation	Remarks
1	Fresh sample	
2	Different high doses to different batches in range 1 to 21 kGy	
3	Preheat 260°C (10s)	
4	Test dose (TD1) 21 Gy	
5	TL 450°C (@ 2°C/s)	TL1 (recording the zero glow 110°C and first glow 340-380°C peak signal)
6	Test dose (TD2) 21 Gy	
7	TL 450°C (@2°C/s)	TL2 (recording the second glow 110°C peak signal)

637

638

639 Table 4: Protocol to measure the HRpDs response of various peaks of quartz in different
640 wavelength range.

Step no.	Operation	Remarks
1	Fresh sample (8 Batches)	
2	Different high doses to different batches in range 1 to 21 kGy	X-axis
3	TL 450°C (@ 2°C/s)	
4	Same test dose 34 Gy to all aliquot	
5	TL 450°C (@ 2°C/s)	Y-axis (Observations using different detection filters)

641

642

643

644 **Figures**

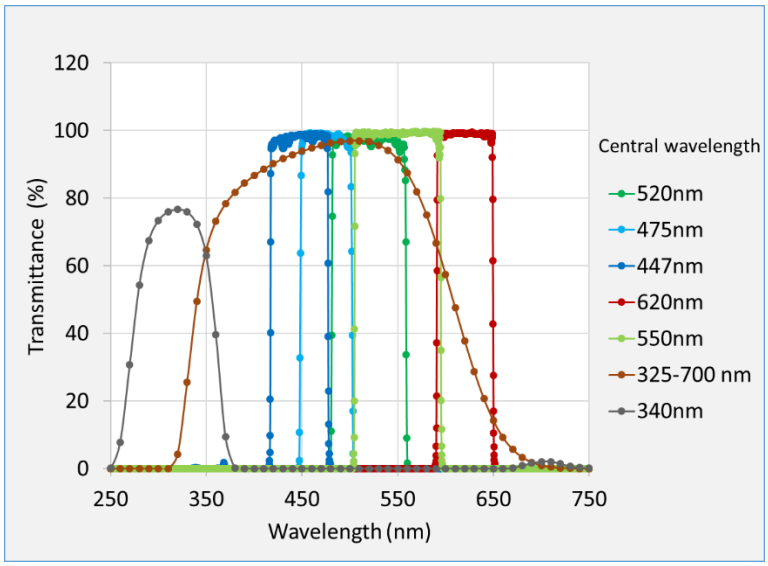

645

646 Fig. 1: The intensity transmittance of various optical band pass filters used in the study. (Data
647 obtained from official website of the filter supplying companies, i.e., www.schott.com,
648 https://hoyafilter.com/, www.edmundoptics.in)

649

650

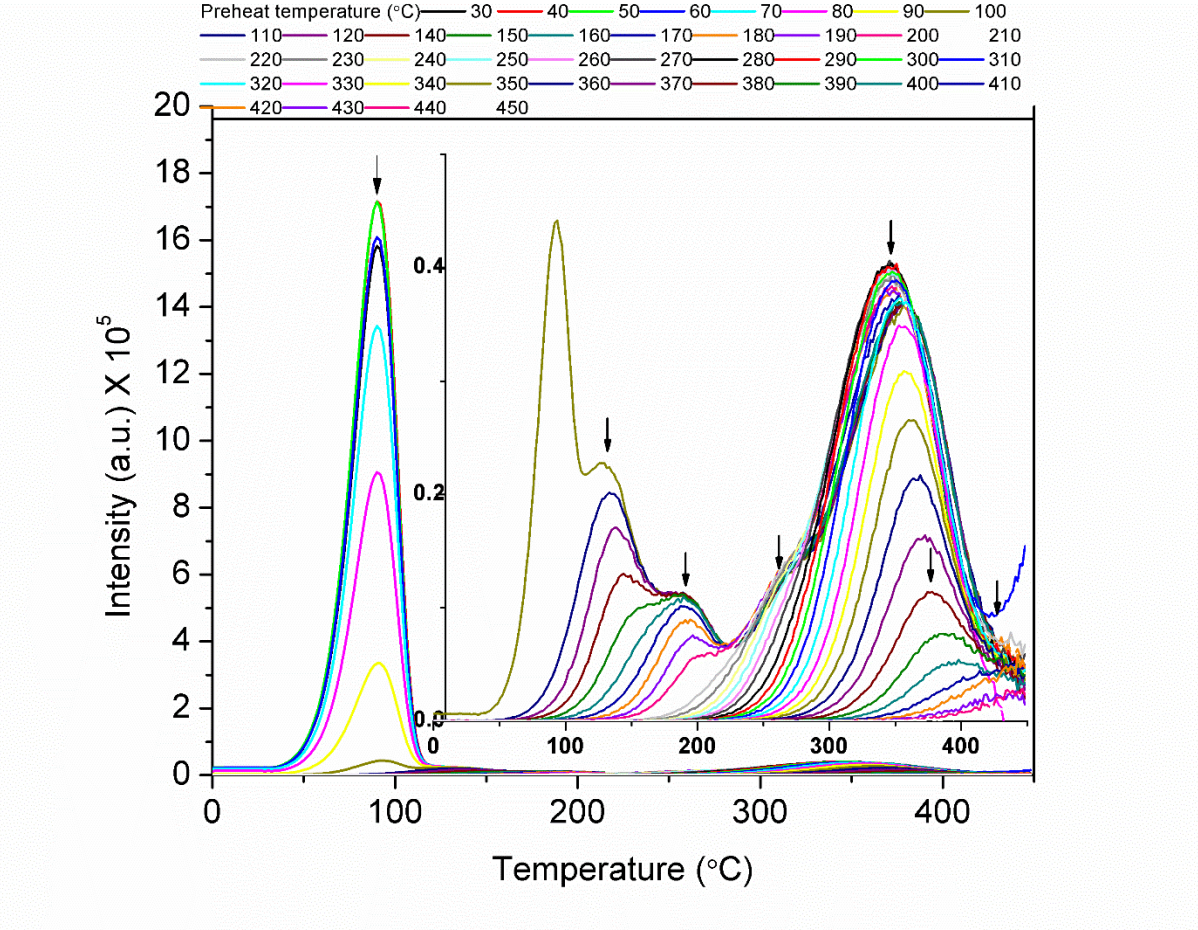

Fig. 2: TL glow curves of sample YS-5 recorded after various preheat temperatures. A dose of 50 Gy is given in each cycle. The visibly distinct peaks are marked by black arrow, emission 325-700nm.

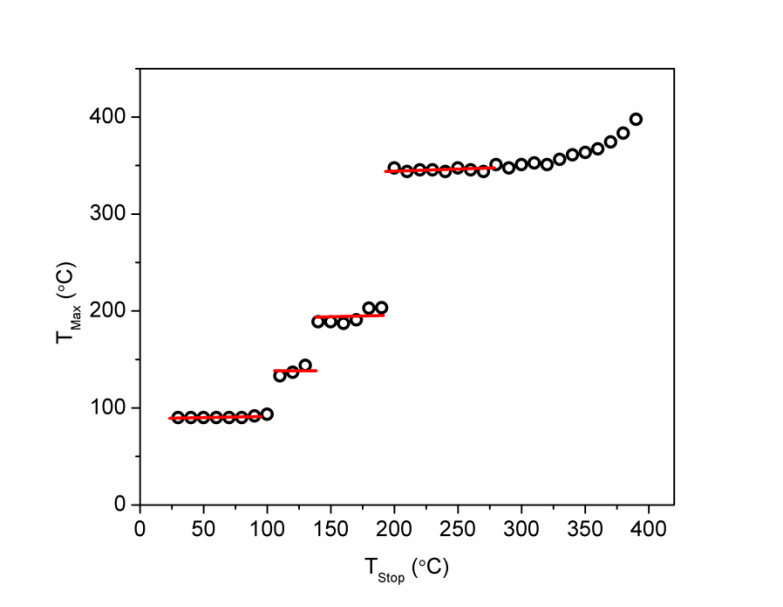

656

657 Fig. 3: T_{max}-T_{stop} graph for sample YS-5, Dose 50 Gy, emission 325-700nm.

658

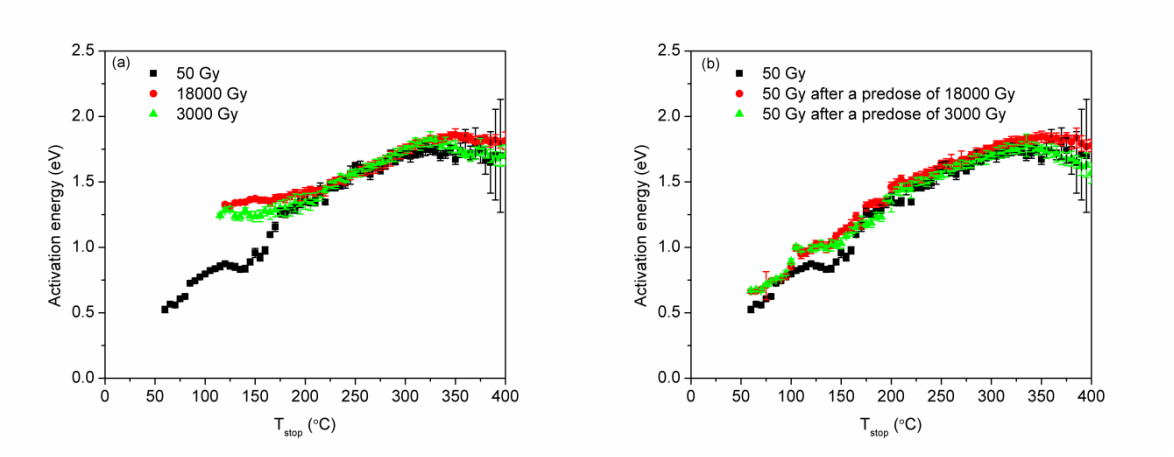

659

660 Fig. 4: Activation energy of sample YS-5 (a) at different doses, (b) at 50 Gy dose but after
661 different HRpD removed by heating upto 450°C, emission 325-700 nm.

662

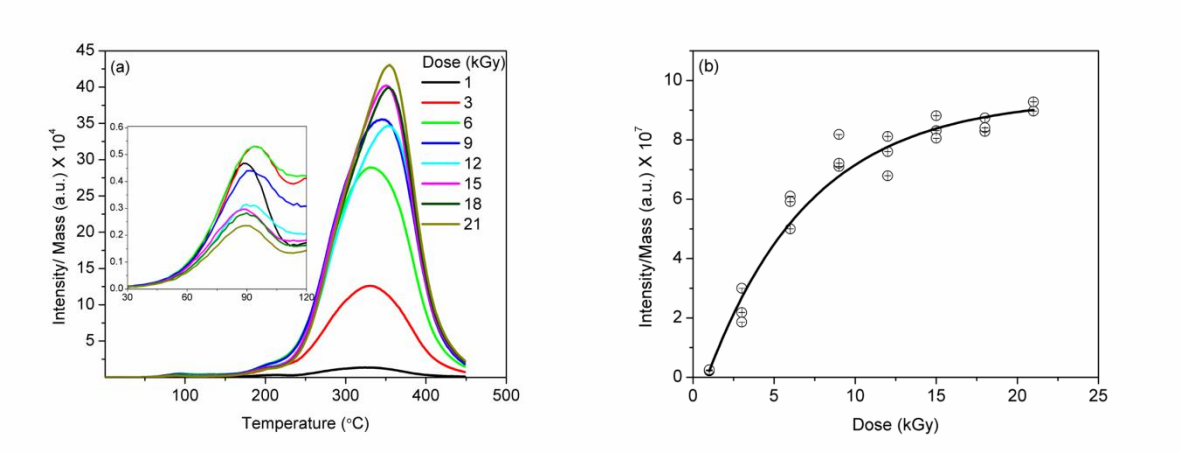

663

664 Fig. 5: a) Thermoluminescence glow curves of sample YS-5 (sedimentary quartz sample) at
665 various high doses in spectral range 325-700 nm. b) Dose response curve of peak from
666 temperature 340-380°C, normalized by the mass. The $2D_0$ value is 11 ± 1 kGy. Each TL glow
667 curve for a given dose is obtained by point wise averaging of three aliquots.

668

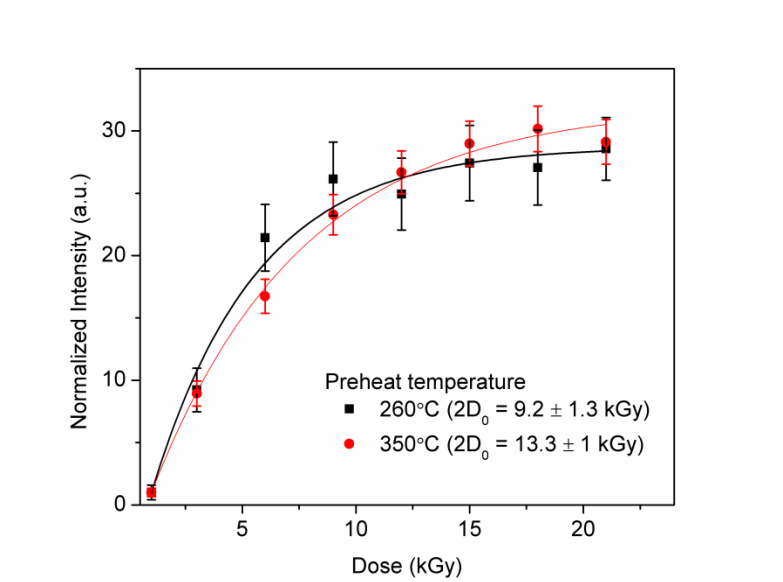

669

670 Fig. 6: DRC of sample YS-5 for different preheat. Intensity is integrated from 250°C-450°C
671 and is normalized by mass and counts corresponding to 1kGy dose in both case. Each point in
672 graph is an average of measurement on 3 aliquots.

673

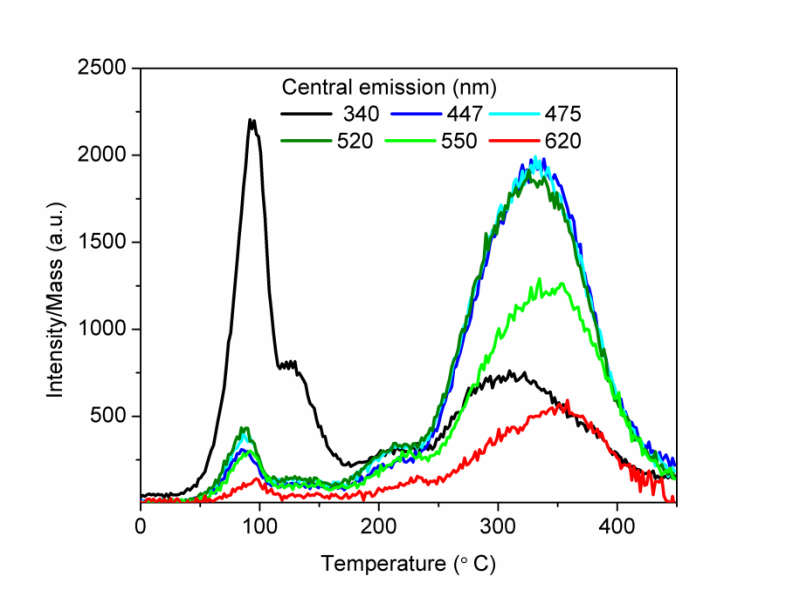

674

675 Fig. 7: TL glow curves of sample YS-5 in different emission bands. An irradiation of 1000
676 Gy is given and on measurement after a preheat of 260°C, 10 s, a small dose of 21 Gy is
677 given for zero glow normalization. The intensity of the curves are not to be compared,
678 because of differences in transmitivity, PMT efficiency and diameter of the filters.

679

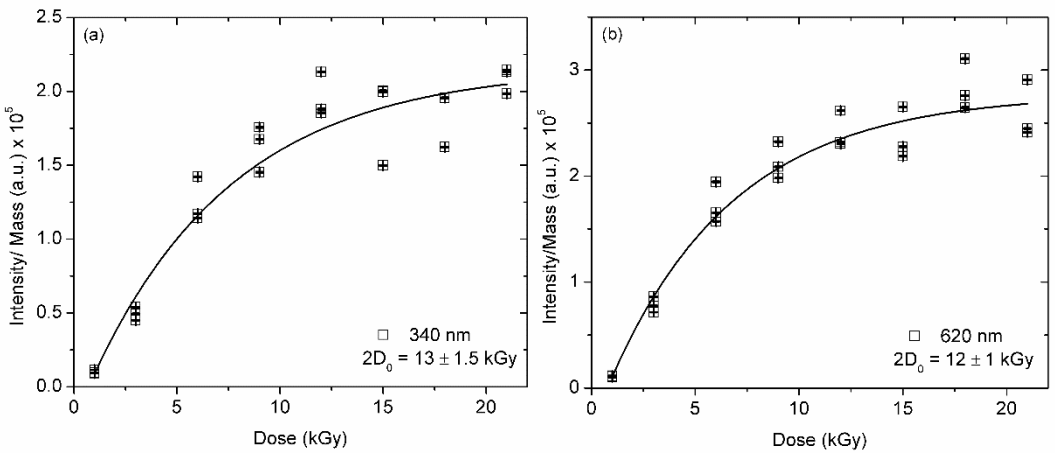

680

681 Fig. 8: The dose response curves of sample YS-5 in UV and red spectral windows of 340-
682 380°C peak, normalized by mass.

683

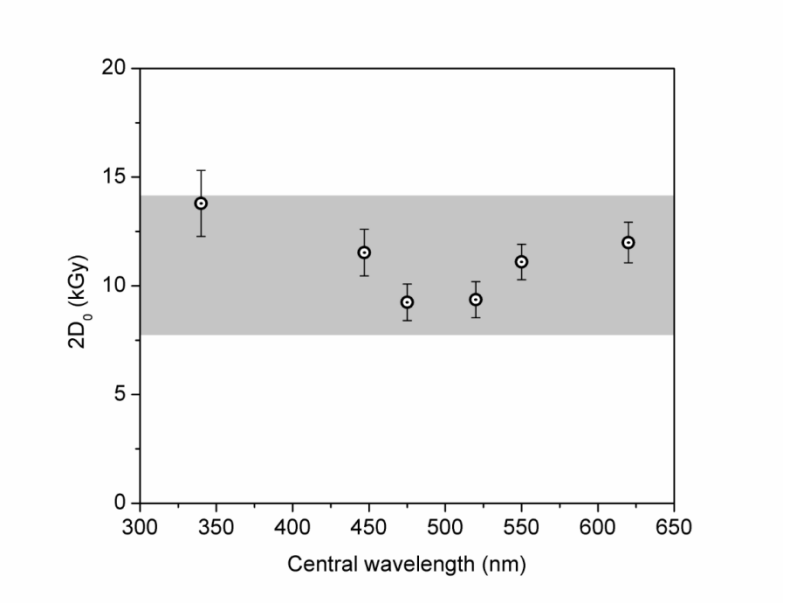

684

685 Fig. 9: Plot of saturation dose ($2D_0$ (kGy)) with TL central emission wavelength for YS-5.

686

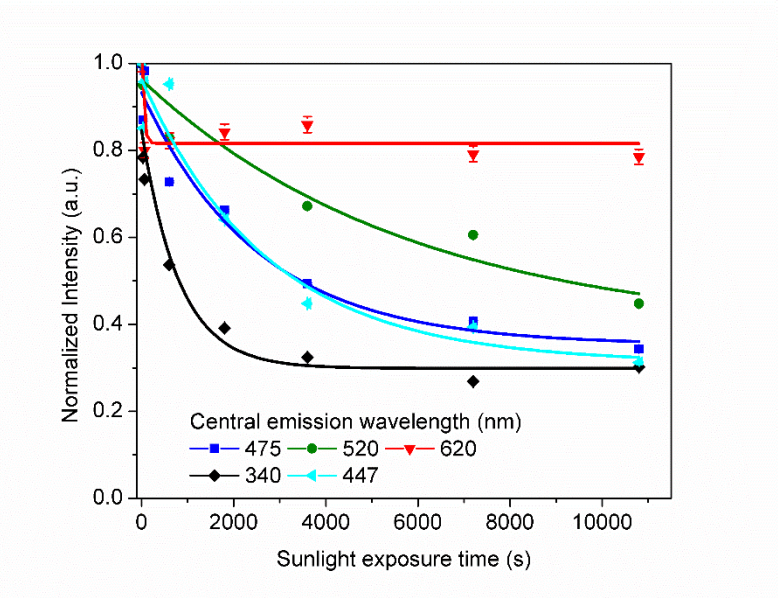

687

688 Fig. 10: Signal bleachability of 340-380°C region, of sample KG-1 exposed to sunlight for
689 different time period.

690

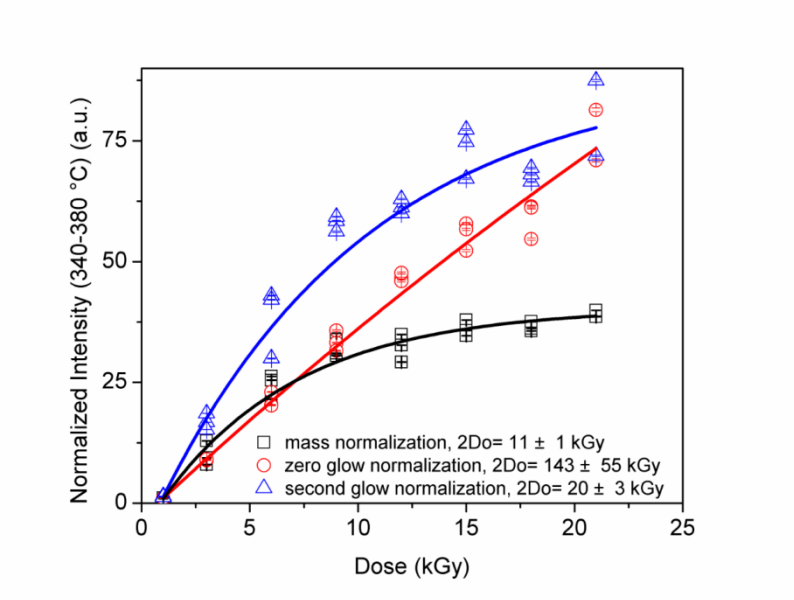

691

692 Fig. 11: Dose response curve of sample YS-5 with different normalization technique. The
693 counts are integrated from 340- 380°C temperature range. The graph has been normalized by
694 the counts of 1 kGy dose.

695

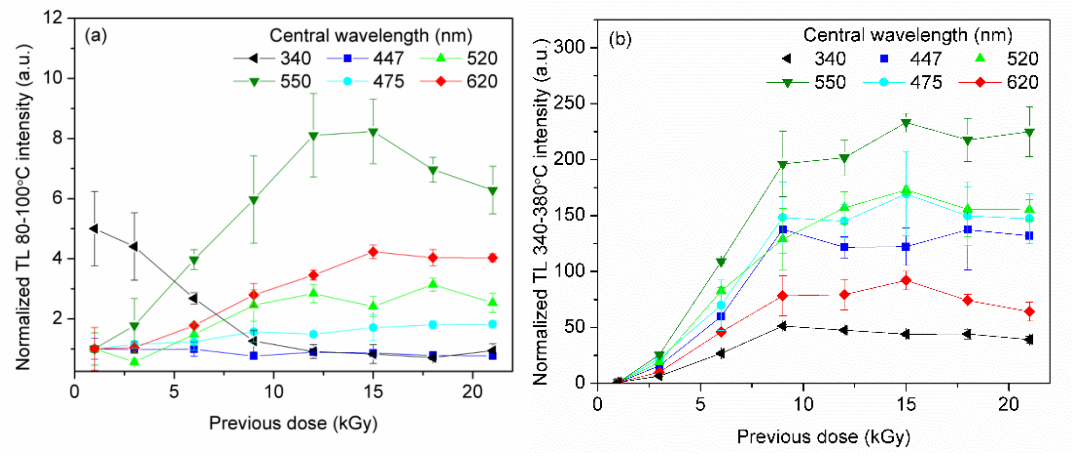

696

697 Fig. 12: The response of sample RQ-1 (a) 80-100 °C peak counts (b) 340-380°C peak counts,
698 to a test dose of 34 Gy after the previous high dose was followed by heating to 450 °C as per
699 table 4. The legends give the emission in different filters which are given in table 2.

700

701

Supplementary Material

1. Position of YS-5 low temperature peak

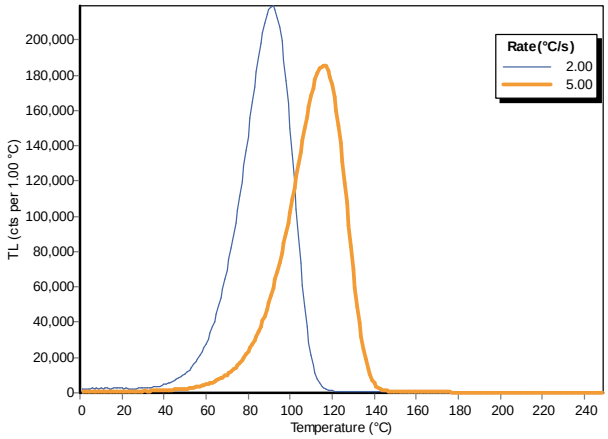

Fig. S1: Shifting of 110°C peak of YS-5 with change in heating rate.

2. Dose response characteristics

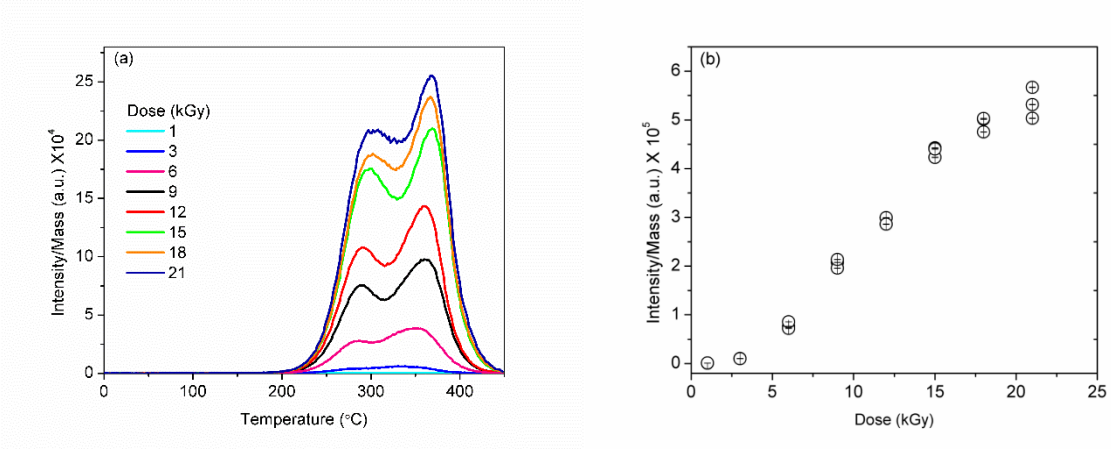

Fig. S2: (a) Thermoluminescence glow curves of sample RQ-1 (rock quartz sample) at various high doses in spectral range 325-700 nm. b) Dose response curve of peak from temperature 340-380°C, normalized by the mass. Each TL glow curve for a given dose is obtained by point wise averaging of three aliquots.

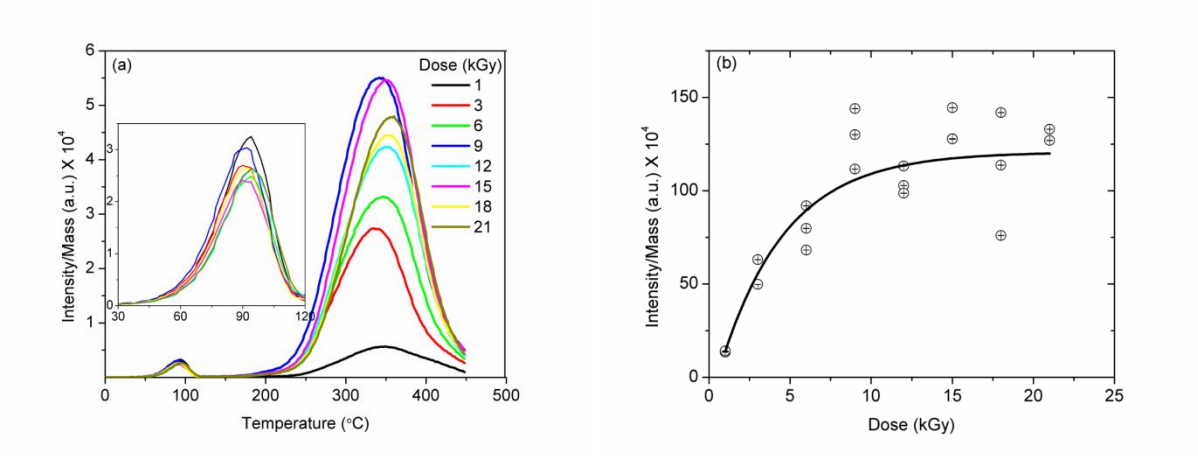

712

713 *Fig. S3: a) Thermoluminescence glow curves of sample SR-23 (sedimentary quartz sample)*
714 *at various high doses in spectral range 325-700 nm. b) Dose response curve of peak from*
715 *temperature 340-380°C, normalized by the mass. The $2D_0$ value is 8.12 ± 1.8 kGy. Each TL*
716 *glow curve for a given dose is obtained by point wise averaging of three aliquots.*

717

718

719 3. Thermoluminescence glow curves after 21 Gy dose

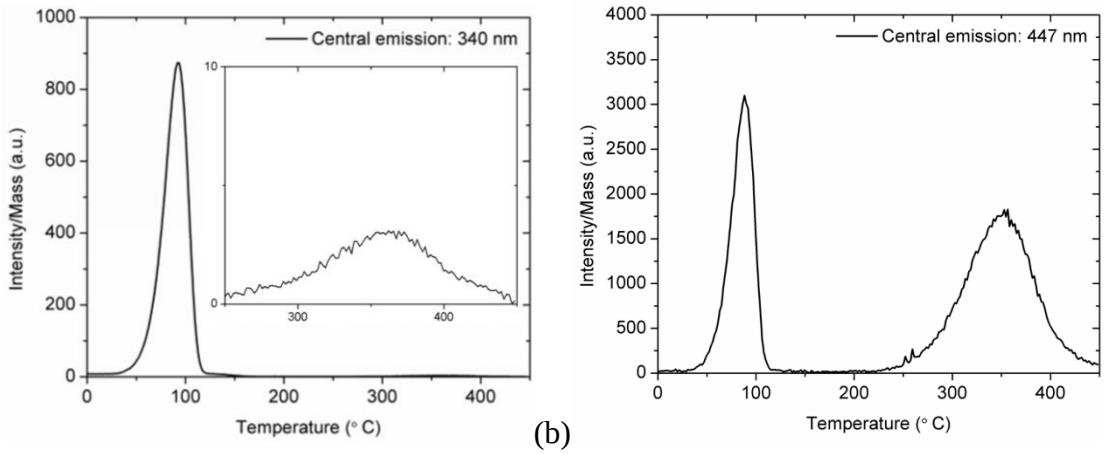

720 (a) (b)

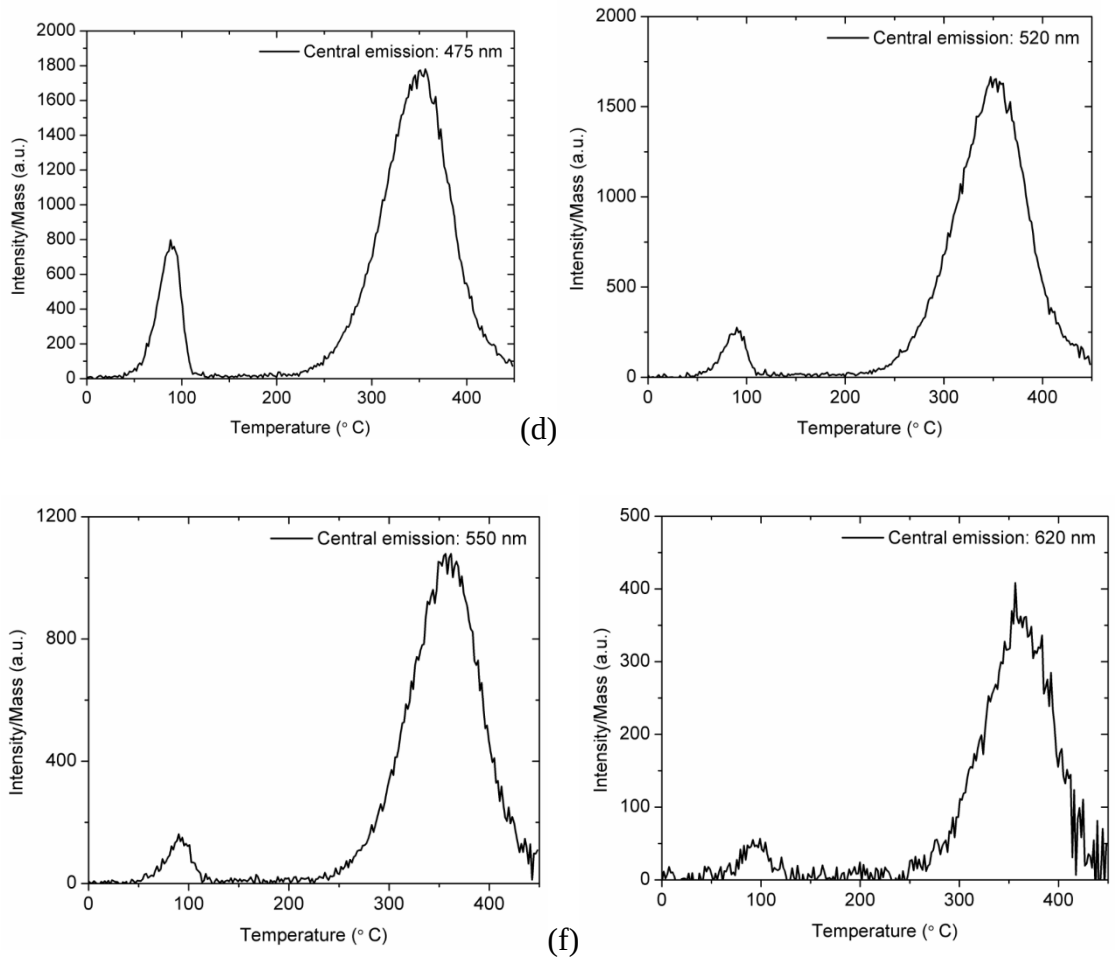

Fig. S4: Thermoluminescence glow curves of sample YS-5 in different emissions. An irradiation of 21 Gy is given. The aliquot was previously irradiated with 1000 Gy. The central wavelength of emissions are (a) 340 nm (b) 447 nm (c) 475 nm (d) 520 nm (e) 550 nm (f) 620 nm.

4. Dose response curves of YS-5 in different spectral filter

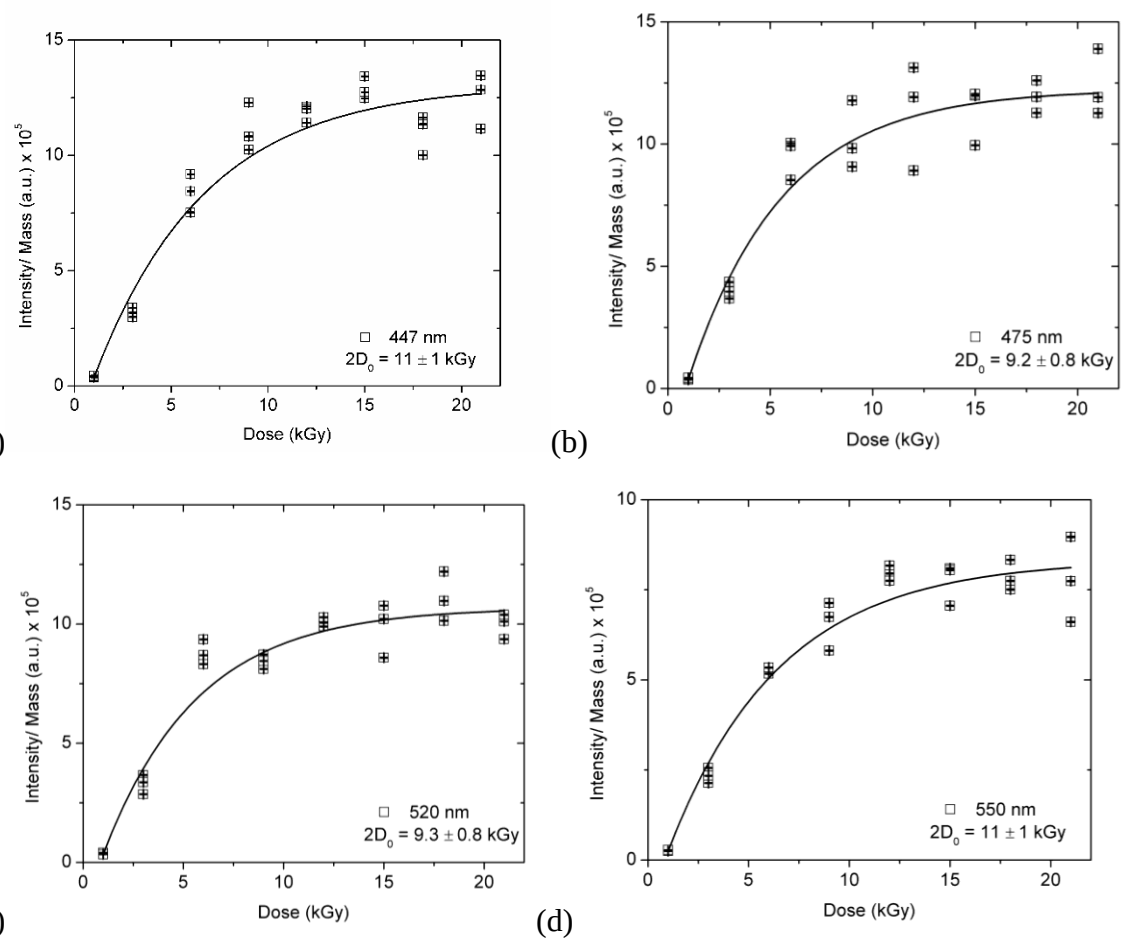

(a) (b)

(c) (d)

Fig. S5: DRC of YS-5 in different spectral window.

5. Multispectral Dose Response Curve of RQ-1

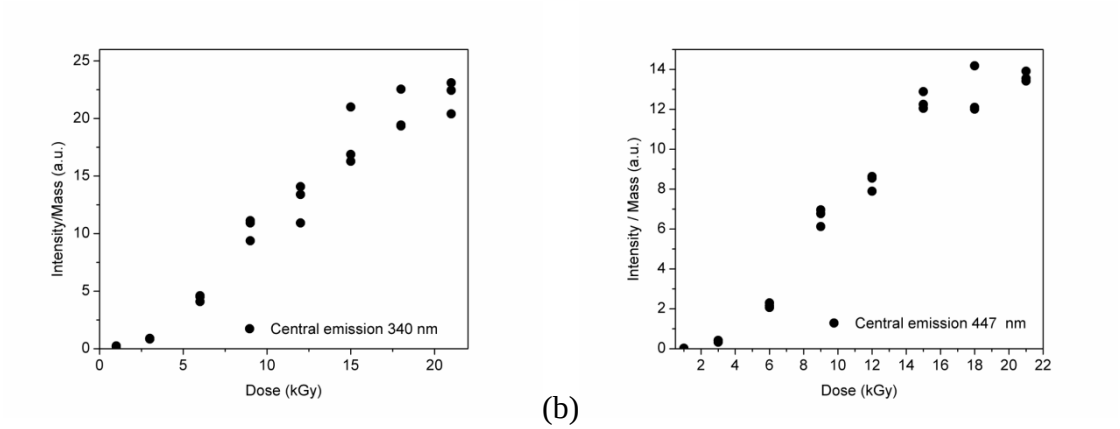

736 (a) (b)

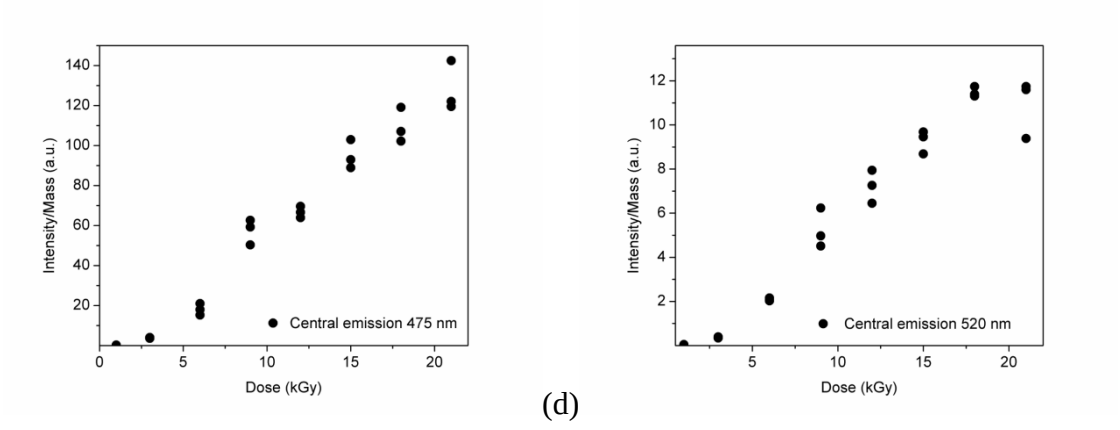

737 (b) (d)

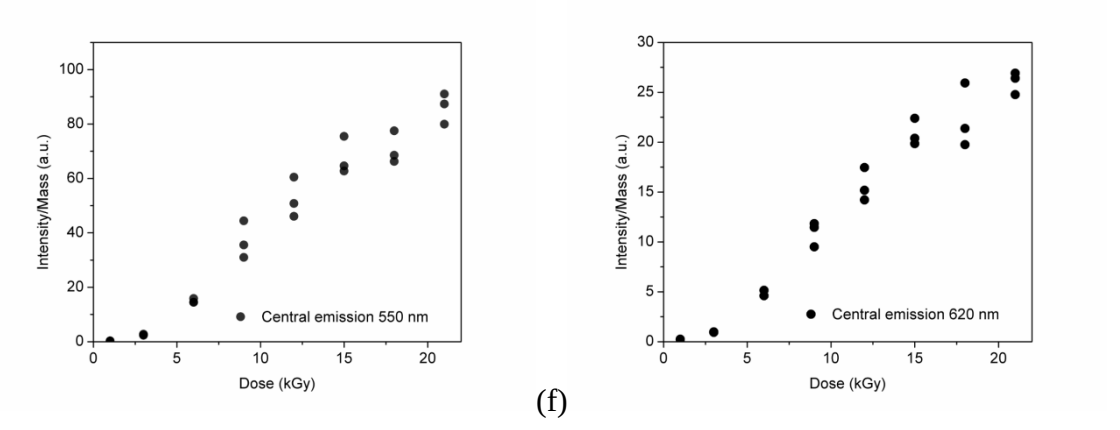

738 (e) (f)

739

740 *Fig. S6: The dose response of sample RQ-1 in multispectral emissions*

741

742 **6. Bleachability of KG1**

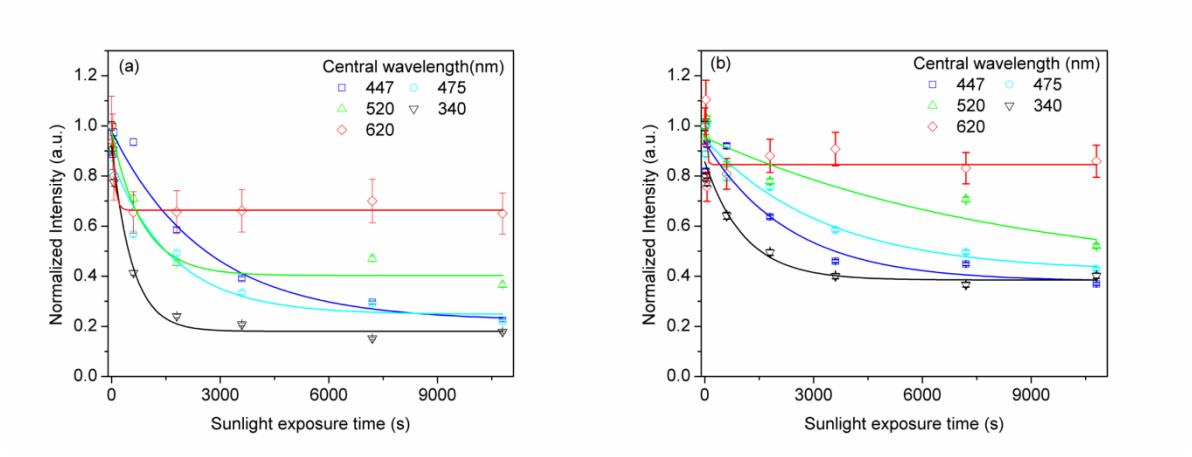

743

744 *Fig. S7: Signal bleachability of (a) 320-330°C region, (b) 370-380°C peak, of sample KG-1*
745 *exposed to sunlight for different time period.*

746

747 7. Dose response curve in multiple spectral emissions

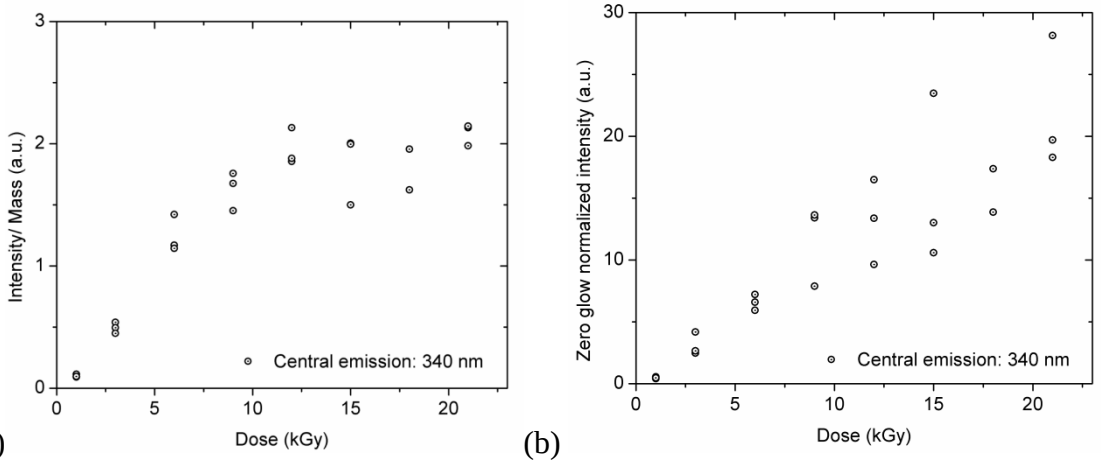

748 (a) (b)

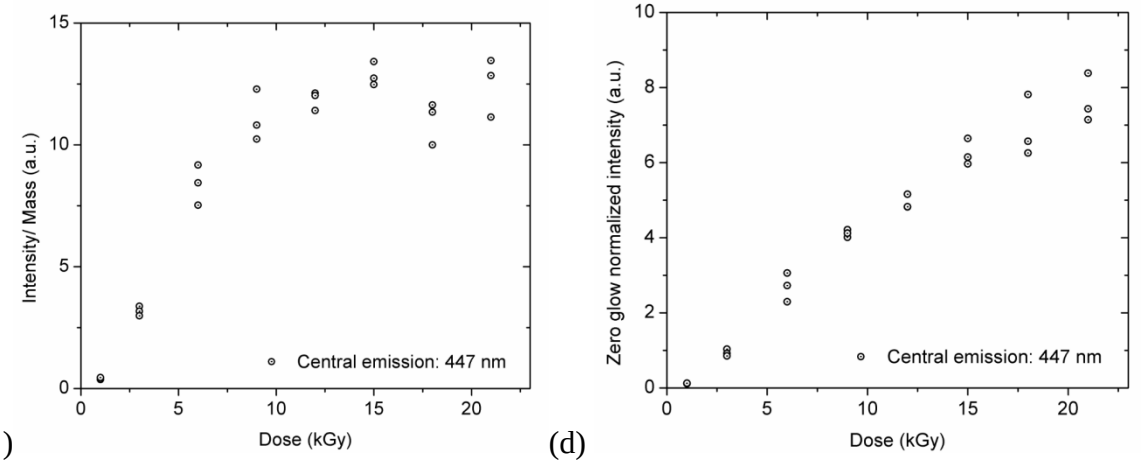

749 (c) (d)

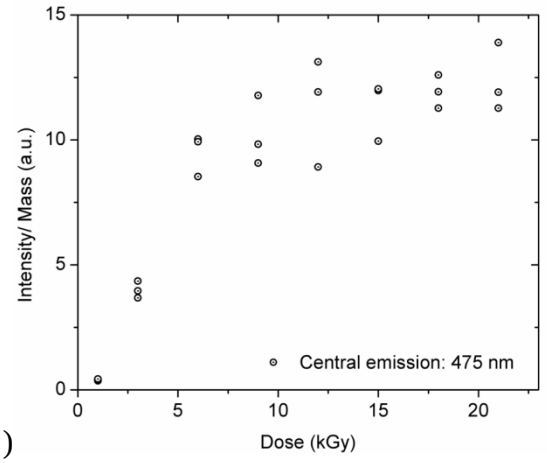
Intensity/ Mass (a.u.)
Dose (kGy)
Central emission: 475 nm

(e)

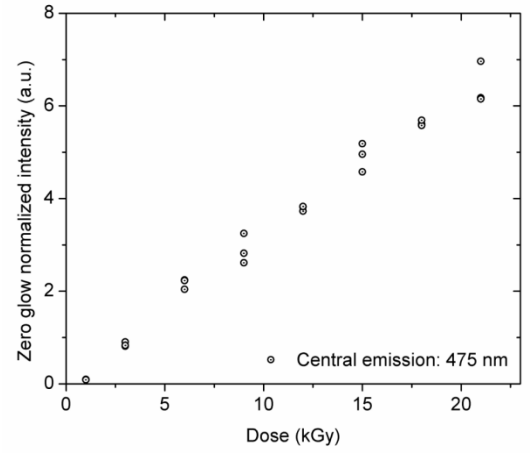
Zero glow normalized intensity (a.u.)
Dose (kGy)
Central emission: 475 nm

(f)

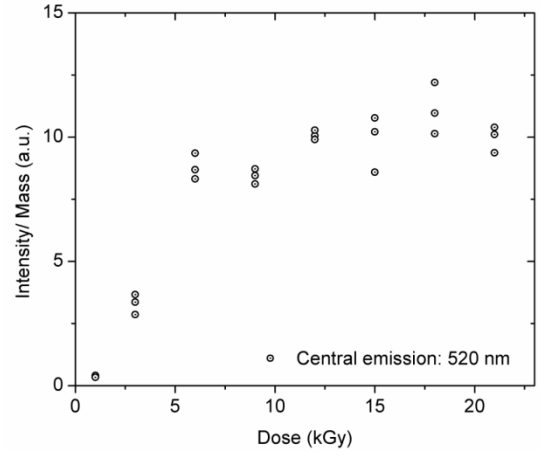
Intensity/ Mass (a.u.)
Dose (kGy)
Central emission: 520 nm

(g)

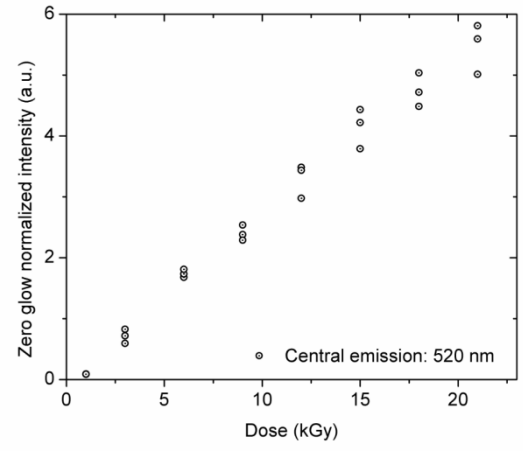
Zero glow normalized intensity (a.u.)
Dose (kGy)
Central emission: 520 nm

(h)

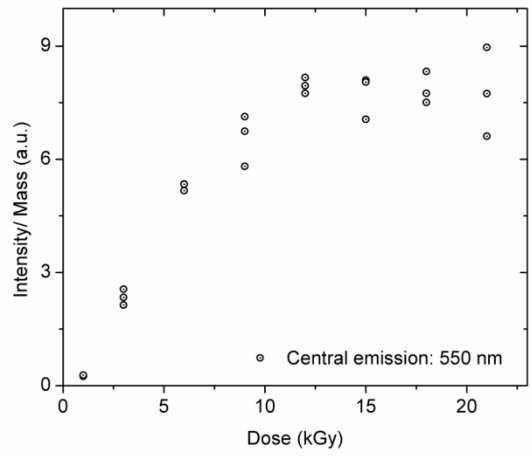
Intensity/ Mass (a.u.)
Dose (kGy)
Central emission: 550 nm

(i)

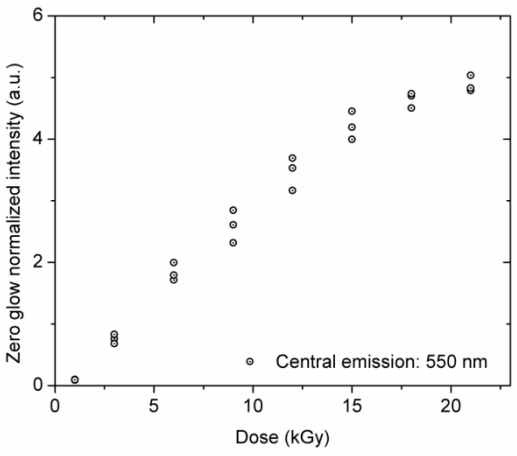
Zero glow normalized intensity (a.u.)
Dose (kGy)
Central emission: 550 nm

(j)

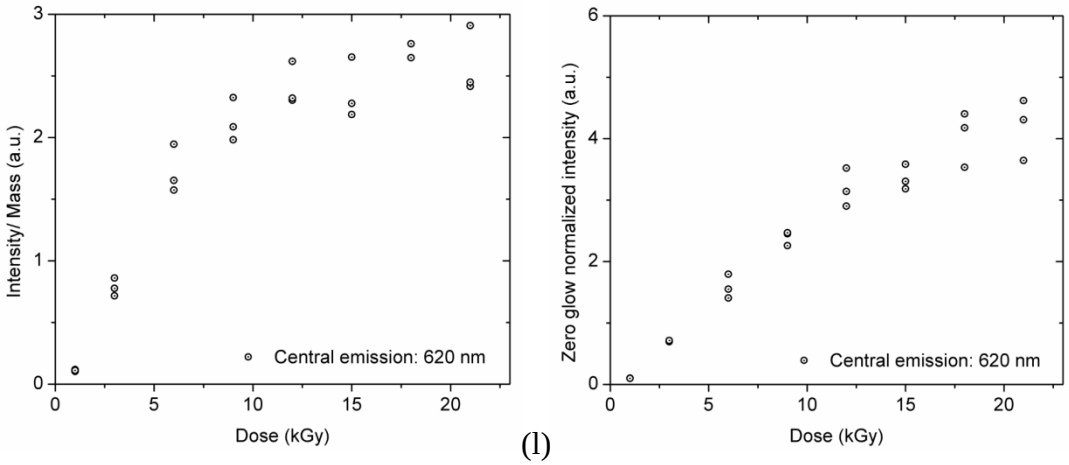

(k) (l)

Fig. S8: The dose response curve of sample YS-5 at high doses in different luminescence emissions. The graphs a,c,e,g,i and k are mass normalized, whereas the graphs b,d,f,h, j and l are zero glow normalized.